

## RESEARCH ARTICLE

10.1029/2017JG004282

## Key Points:

- A mechanistic description of tropical leaf phenology for ecosystem models is presented
- Model simulations for 32 sites in the Amazon realistically reproduce carbon/water fluxes
- Leaf phenology explains dry-season greening with little impact on evapotranspiration fluxes

## Supporting Information:

- Supporting Information S1

## Correspondence to:

G. Manoli,  
manoli@ifu.baug.ethz.ch

## Citation:

Manoli, G., Ivanov, V. Y., & Fatichi, S. (2018). Dry-season greening and water stress in Amazonia: The role of modeling leaf phenology. *Journal of Geophysical Research*, 123, 1909–1926. <https://doi.org/10.1029/2017JG004282>

Received 7 NOV 2017

Accepted 21 MAY 2018

Accepted article online 29 MAY 2018

Published online 16 JUN 2018

## Dry-Season Greening and Water Stress in Amazonia: The Role of Modeling Leaf Phenology

Gabriele Manoli<sup>1</sup> , Valeriy Y. Ivanov<sup>2</sup> , and Simone Fatichi<sup>1</sup> 

<sup>1</sup>Institute of Environmental Engineering, ETH Zurich, Zurich, Switzerland, <sup>2</sup>Department of Civil and Environmental Engineering, University of Michigan, Ann Arbor, MI, USA

**Abstract** Large uncertainties on the sensitivity of Amazon forests to drought exist. Even though water stress should suppress photosynthesis and enhance tree mortality, a green-up has been often observed during the dry season. This interplay between climatic forcing and forest phenology is poorly understood and inadequately represented in most of existing dynamic global vegetation models calling for an improved description of the Amazon seasonal dynamics. Recent findings on tropical leaf phenology are incorporated in the state-of-the-art eco-hydrological model Thetys & Chloris. The new model accounts for a mechanistic light-controlled leaf development, synchronized dry-season litterfall, and an age-dependent leaf photosynthetic capacity. Simulation results from 32 sites in the Amazon basin over a 15-year period successfully mimic the seasonality of gross primary productivity; evapotranspiration (ET); as well as leaf area index, leaf age, and leaf productivity. Representation of tropical leaf phenology reproduces the observed dry-season greening, reduces simulated gross primary productivity, and does not alter ET, when compared with simulations without phenology. Tolerance to dry periods, with the exception of major drought events, is simulated by the model. Deep roots rather than leaf area index regulation mechanisms control the response to short-term droughts, but legacy effects can exacerbate multiyear water stress. Our results provide a novel mechanistic approach to model leaf phenology and flux seasonality in the tropics, reconciling the generally observed dry-season greening, ET seasonality, and decreased carbon uptake during severe droughts.

### 1. Introduction

The metabolic rhythm of Amazon rainforests (phenology of vegetation, seasonality of carbon and water fluxes) is a key component of the global carbon cycle (Phillips et al., 2009) with impacts on tropical moist convection (Knox et al., 2011) and important consequences on global climate (Alden et al., 2016; Cox et al., 2000; Huete et al., 2006; Wu et al., 2016). The importance of the Amazon in the Earth system is therefore unquestionable (Davidson et al., 2012; Malhi et al., 2008), but its vulnerability to drought and the risks associated with a drying climate (Ahlström et al., 2017; Malhi et al., 2008; Meir et al., 2009) is unclear, as conflicting results have been reported (Brando et al., 2010).

Dry periods, that is, when precipitation is below potential evapotranspiration, alter forest metabolism. When severe water stress is generated, drought can reduce or reverse the carbon sink (Gatti et al., 2014; Lewis et al., 2011; Phillips et al., 2009) and lead to accelerated forest mortality (da Costa et al., 2010; Lewis et al., 2011; Liu et al., 2018; Malhi et al., 2009; Meir et al., 2009). However, evidence of both positive (e.g., Saleska et al., 2003, 2007) and negative (e.g., Meir et al., 2009; Nepstad et al., 2007) impacts of drought on forest functioning exists. The severe drought event that affected the Amazon basin in 2005 is a clear example of such conflicting results: While Phillips et al. (2009) reported a significant decrease in carbon uptake and concluded that Amazon forests are vulnerable to increasing moisture stress, remote sensing observations revealed a basin-wide increase in photosynthetic activity, suggesting a biome resilience (defined as the capability to sustain carbon/water fluxes during extremely dry periods) higher than originally thought (Ahlström et al., 2017; Saleska et al., 2007).

Such unexpected dry-season greening, associated with an increase in leaf area timed to solar radiation (Huete et al., 2006; Myneni et al., 2007), has been confirmed by a large number of remote sensing, eddy flux tower, and field observations (Brando et al., 2010; Guan et al., 2015; Huete et al., 2006; Hutyrta et al., 2007; Myneni et al., 2007; Morton et al., 2014; Restrepo-Coupe et al., 2013; Saleska et al., 2003, 2007, 2016;

Samanta et al., 2012; Wu et al., 2016), suggesting that light, rather than water, may regulate forest seasonality in tropical wet climates. However, seasonal variations of temperature and radiation are fairly moderate in the tropics and understanding whether the carbon fluxes are controlled by hydro-climate (e.g., Borchert, 1998; Guan et al., 2015) or variations in the forest photosynthetic machinery (leaf area, leaf demography, and photosynthetic capacity; e.g., Brando et al., 2010; Huete et al., 2006; Restrepo-Coupe et al., 2013) has been a subject of debate (Hayek et al., 2018; Liu et al., 2018; Morton et al., 2014; Saleska et al., 2016).

The different theories have been recently reconciled by camera observations and leaf-level measurements revealing a synchronization of dry-season litterfall with the onset of new leaves having higher photosynthetic capacity and therefore light use efficiency (Albert et al., 2018; Wu et al., 2016). Such a coordinated leaf development explains observed seasonal variations of leaf area index (LAI), photosynthetic capacity (PC), and gross primary productivity (GPP), demonstrating that canopy phenology plays an important role in regulating forest fluxes during the dry season (Wu et al., 2016). However, the interplay between phenologic and climatic factors regulating the overall forest response to dry periods and droughts (i.e., during the dry periods of 2005 and 2010; Lewis et al., 2011) is still unclear and the compound effects of leaf phenology and plant water stress on carbon/water fluxes remain elusive, framing the scope here.

The fact that seasonality in photosynthetic capacity is driven by changes in leaf quality and quantity (younger leaves and changes in LAI) can also explain the reported discrepancies between observations and model simulations (Restrepo-Coupe et al., 2017; Wu et al., 2016). Most of existing dynamic global vegetation models, DGVMs (and, similarly, eco-hydrological models, terrestrial biosphere models, and land surface models; Fatichi et al., 2014), assume simple or no phenology for tropical evergreen biomes, and they account for variability of the climate drivers only (Restrepo-Coupe et al., 2017; Wu et al., 2016). Thus, models systematically fail to reproduce the seasonality of carbon fluxes and the observed dry-season greening (Restrepo-Coupe et al., 2017). Tropical forest description in DGVMs has been continuously improved (Baker et al., 2008; Christoffersen et al., 2014; De Weirdt et al., 2012; Galbraith et al., 2010; Ivanov et al., 2012; Kim et al., 2012; Verbeeck et al., 2011; Von Randow et al., 2013), but these models still produce inaccurate GPP predictions at timescales from days to decades (Restrepo-Coupe et al., 2017). Despite limitations in reproducing GPP seasonality, DGVMs generally capture the observed seasonality of ET fluxes and have provided insights into the importance of deep rooting systems, hydraulic redistribution, root niche separation, and groundwater fluxes to explain the observed tolerance of Amazon forests to extended droughts (Baker et al., 2008; Christoffersen et al., 2014; Ivanov et al., 2012; Miguez-Macho & Fan, 2012). Hence, given the assumption of an aseasonal photosynthetic infrastructure, it is unclear whether model simulations provide the right answers for the right reasons (Restrepo-Coupe et al., 2017). Recently, Wu, Serbin, et al. (2017) have proposed a two-fraction leaf (sun/shade), two-layer canopy model for representing tropical photosynthetic seasonality in DGVMs, and Xu et al. (2017) have shown that cross-species variations in leaf longevity can be explained by a trait-driven carbon optimality model. However, the impact of such dynamics on carbon/water relations was not addressed, leaving the following questions open: (i) What is the impact of leaf phenology on ecosystem carbon and water fluxes in the Amazon basin? (ii) Does photosynthetic seasonality enhance or decrease forest resilience to drought? (iii) Is the accuracy of model simulations, in terms of carbon and water fluxes, different when the forest photosynthetic machinery is allowed to vary seasonally?

To answer these questions a novel eco-hydrological model description of phenology in tropical biomes is developed here and used to investigate carbon and water fluxes seasonality across the Amazon basin. The specific approaches of this study are as follows: (i) the development of a mechanistic light-controlled leaf phenology model for tropical evergreen forests based on recent experimental observations, (ii) the use of model simulations to assess the impact of leaf phenology on the seasonality of biosphere-atmosphere exchanges in the Amazon, and (iii) a multisite and multiyear analysis of water/carbon fluxes to evaluate the interplay between leaf phenology and water stress controls on forest responses to dry periods.

In summary, given the projected increase in the Amazonian dry-season length towards the end of this century (Boisier et al., 2015; Fu et al., 2013; Lintner et al., 2012; Malhi et al., 2008; Marengo et al., 2011), the need of realistically describing biosphere-atmosphere interactions under future climate (Fatichi, Pappas, et al., 2016), and the fact that tropical leaf phenology is not accounted for in the existing DGVMs (Restrepo-Coupe et al., 2017; Wu et al., 2016), the overarching goal of this study is to improve the representation of water/carbon fluxes in the tropics, quantify the role of photosynthetic seasonality, and disentangle the role of between phenology and water stress.

## 2. Materials and Methods

### 2.1. Study Sites

Local observations from 32 tropical forest sites in the Amazon basin are considered here (Table 1). Flux tower data for six sites (Bananal, CAX, km34, km67, km83, and RJA) are obtained from the LBA-ECO Flux Tower Network Data Compilation and LBA-Model Intercomparison Project (Christoffersen et al., 2014; De Gonçalves et al., 2013; Restrepo-Coupe et al., 2013), freely available online ([ftp://saleskalab.eebweb.arizona.edu/pub/BrasilFlux\\_Data/](ftp://saleskalab.eebweb.arizona.edu/pub/BrasilFlux_Data/)). Additional meteorological data (temperature, precipitation, relative humidity, radiation, pressure, and wind speed) from eight LBA-ECO weather stations (Belterra, Embrapa, Guarana, Jamaraua, km117, Mojui, Sudam, and Vilafranca; Fitzjarrald et al., 2008) and 18 meteorological stations (A101, A109–113, A117, A120–126, A128, and A133–134) run by the Brazilian Meteorological Institute, INMET (Instituto Nacional de Meteorologia-Ministério da Agricultura, Pecunária e Abastecimento) are also used as input for model simulations (see next subsections). Overall, LBA-ECO data are available for the period 1999–2006, while INMET meteorological stations cover the period 2008–2015 with site A101 spanning from 2000 to 2014.

Solar-induced fluorescence (SIF) observations from the Global Ozone Monitoring Instrument 2 (GOME-2) are also used to assess model performance (monthly data at a spatial resolution of  $0.5^\circ \times 0.5^\circ$  (Joiner et al., 2013)). SIF has been shown to provide good estimates of GPP (e.g., Yang et al., 2015; Zhang, Guanter, et al., 2016; Zhang, Xiao, et al., 2016) and forest response to drought (e.g., Joiner et al., 2013; Lee et al., 2013). For instance, SIF correlates with GPP at diurnal and seasonal scales (with  $r^2$  values larger than 0.7 for spring and summer season in North America; Zhang, Xiao, et al., 2016), thus providing an additional piece of information to evaluate the seasonality of carbon fluxes at the study sites.

### 2.2. Model Formulation

#### 2.3. Phenological Metrics

Seasonal observations of GPP, LAI, photosynthetic capacity, and new leaf production at sites km34 and km67 have been digitized from (Wu et al., 2016; Figure 1). Photosynthetic efficiency  $e_{rel}$  is estimated from PC data as  $e_{rel} = PC/PC_{max}$ , with PC being the canopy photosynthesis per unit incoming light under reference climatic conditions (Wu et al., 2016), which can be interpreted as a metric of the ecosystem-scale photosynthetic capacity (Wu, Guan, et al., 2017), and  $PC_{max}$  is the annual maximum of PC. The partitioning of total LAI ( $m_{leaf}^2 \cdot m_{ground}^{-2}$ ) into young, mature, and old leaves presented by Wu et al. (2016) is used to estimate the average leaf age  $A_L$  [mo] and the fraction of new leaves (see Figures 1b and 1c for details). Note that  $A_L$  in the model is prognostically estimated and represents the average of the entire canopy, since the model does not track different leaf cohorts (see next subsections). The observations show consistent seasonal patterns at both sites (Figures 1b–1e) with increased leaf production at the end of the wet season, followed by leaf rejuvenation and an increase in photosynthetic capacity as the dry season develops. Specifically, the peak of new leaf production and the minimum leaf age occur during the dry season over a span of 1–2 months (Figures 1c–1e), while the largest PC is obtained for mature leaves (i.e., intermediate age at the end of dry season, see also model simulations in the supporting information), as young and old leaves are less photosynthetically efficient (Wu et al., 2016).

Combining such leaf production data with estimated canopy leaf age and observed photosynthetic capacity provides a two-dimensional relation for  $e_{rel}$  (Figure 1f):

$$e_{rel}(A_L, f_{NL}) = 1.61 - 0.06 \cdot A_L - 1.20 \cdot f_{NL} \quad (1)$$

where the coefficients have been estimated by a least-square fit of the data,  $f_{NL} = k_c \frac{NB_L^*}{LAI}$  [ $mo^{-1}$ ] is the monthly fraction of newly generated leaves (i.e. age <1 month) acting to decrease  $e_{rel}$ ,  $NB_L^*$  is the new leaf production ( $m^2 \cdot m^{-2} \cdot mo^{-1}$ ; as observed by Wu et al., 2016) and  $k_c$  is a correction factor to ensure consistency between  $NB_L^*$  and LAI. Specifically,  $k_c = \frac{d_{leaf} \cdot LAI}{\sum NB_L^*}$ , where  $\overline{LAI}$  is the mean annual LAI,  $d_L$  is the turnover rate of green aboveground biomass from litterfall estimates [ $mo^{-1}$ ] and  $NB_L^*$  is summed over a year. Note that  $k_c$  is introduced here to preserve consistency (mass conservation) between observations of standing LAI, annual litterfall, and monthly leaf biomass production estimates (Figure 1e), which indicate that leaf average turnover is about 270 days. In the case of model simulations carbon mass is conserved and therefore  $k_c = 1$ . Given that equation (1) admits values above 1, a limit  $e_{rel} \leq 1$  is imposed (Figure 1f). The overall good fit of equation (1) ( $R^2 = 0.93$ ) with data reveals a linear dependence of photosynthetic capacity on canopy leaf age and the fraction of new leaves (in accordance with the results by Wu, Serbin, et al., 2017, and Xu et al., 2017).

**Table 1**

Name and Location of the Study Sites, Mean Annual Precipitation (MAP), Number of Dry Months  $n_{dry}$  (i.e., Monthly Precipitation < 100 mm), and Monitoring Method

Site	Latitude	Longitude	MAP (mm/year)	$n_{dry}$	Monitoring method	References
A101–134 (18 sites)	[−8.76; −0.11]	[−69.86; −56.75]	1738–3223	0–4	Meteo station	Instituto Nacional de Meteorologia, Brazil
Bananal	−9.82	−50.16	1,714	6	Flux tower	De Gonçalves et al. (2013); Restrepo-Coupe et al. (2013); Christoffersen et al. (2014)
Belterra	−2.64	−54.94	1,642	6	Meteo station	Fitzjarrald et al. (2008)
Caxiuana (CAX)	−1.72	−51.47	2,022	4	Flux tower	Restrepo-Coupe et al. (2013)
Embrapa	−2.39	−54.33	2,411	8	Flux tower	—
Guarana	−2.68	−54.32	1,579	6	Meteo station	Fitzjarrald et al. (2008)
Jamaraqua	−2.81	−55.04	1,590	7	Meteo station	Fitzjarrald et al. (2008)
km34 (Manaus)	−2.61	−60.21	2,735	2	Flux tower	De Gonçalves et al. (2013); Restrepo-Coupe et al. (2013); Christoffersen et al. (2014)
km67 (Santarem)	−2.86	−54.96	1,649	5	Flux tower	De Gonçalves et al. (2013); Restrepo-Coupe et al. (2013); Christoffersen et al. (2014)
km83 (Santarem)	−3.02	−54.96	1,716	5	Flux tower	De Gonçalves et al. (2013); Restrepo-Coupe et al. (2013); Christoffersen et al. (2014)
km117	−3.35	−54.92	1,356	6	Meteo station	Fitzjarrald et al. (2008)
Mojui	−2.77	−54.58	1,618	5	Meteo station	Fitzjarrald et al. (2008)
Reserva Jaru (RJA)	−10.08	−61.93	2,325	5	Flux tower	De Gonçalves et al. (2013); Restrepo-Coupe et al. (2013); Christoffersen et al. (2014)
Sudam	−2.54	−54.09	1,278	7	Meteo station	Fitzjarrald et al. (2008)
Vilafranca	−2.35	−55.03	2,367	4	Meteo station	Fitzjarrald et al. (2008)

Specifically,  $e_{rel}$  is maximum at an average leaf age of 8–9 months given that the carbon assimilation rates are low for young leaves and reach a peak at maturity before decreasing with age (Wu, Serbin, et al., 2017; Xu et al., 2017).

Equation (1) provides a simple description of phenology-driven changes in PC, explaining the role of quality (age) in regulating seasonal carbon fluxes. To include this information into models that use an aseasonal photosynthetic scheme, the maximum Rubisco capacity can be modified as follows:

$$V_{c,max25}^* = V_{c,max25} \cdot e_{rel}(A_L, f_{NL}) \quad (2)$$

where  $V_{c,max25}$  is the maximum Rubisco capacity at 25°C and  $e_{rel}$  is the photosynthetic efficiency defined according to equation (1), but computed with simulated quantities (i.e.,  $A_L$ ,  $LAI$ , and  $NB_L^*$ ).

### 2.3.1. T&C Model

To simulate soil water dynamics and vegetation functioning, the eco-hydrological model T&C is used (Fatichi, 2010; Fatichi et al., 2012a, 2012b). T&C combines a dynamic vegetation model accounting for plant physiology, phenology, and carbon pool dynamics with a land surface and hydrologic module solving the surface energy balance, soil-vegetation-atmosphere exchanges and subsurface water dynamics. T&C does not use plant functional types, and its vegetation parameterization is tailored to each site and potentially for multiple species at each site, even though many parameters may be equal across species and sites (Fatichi, Leuzinger, et al., 2016; Mastrotheodoros et al., 2017). The T&C model can be thus listed as a trait-based vegetation model accounting for interspecific and intraspecific plant trait variability. Trait-based approaches typically offer a better representation of ecosystem functioning than models grouping plant traits into broad categories (Pappas et al., 2016). T&C has been successfully applied to simulate water and carbon fluxes in various ecosystems worldwide

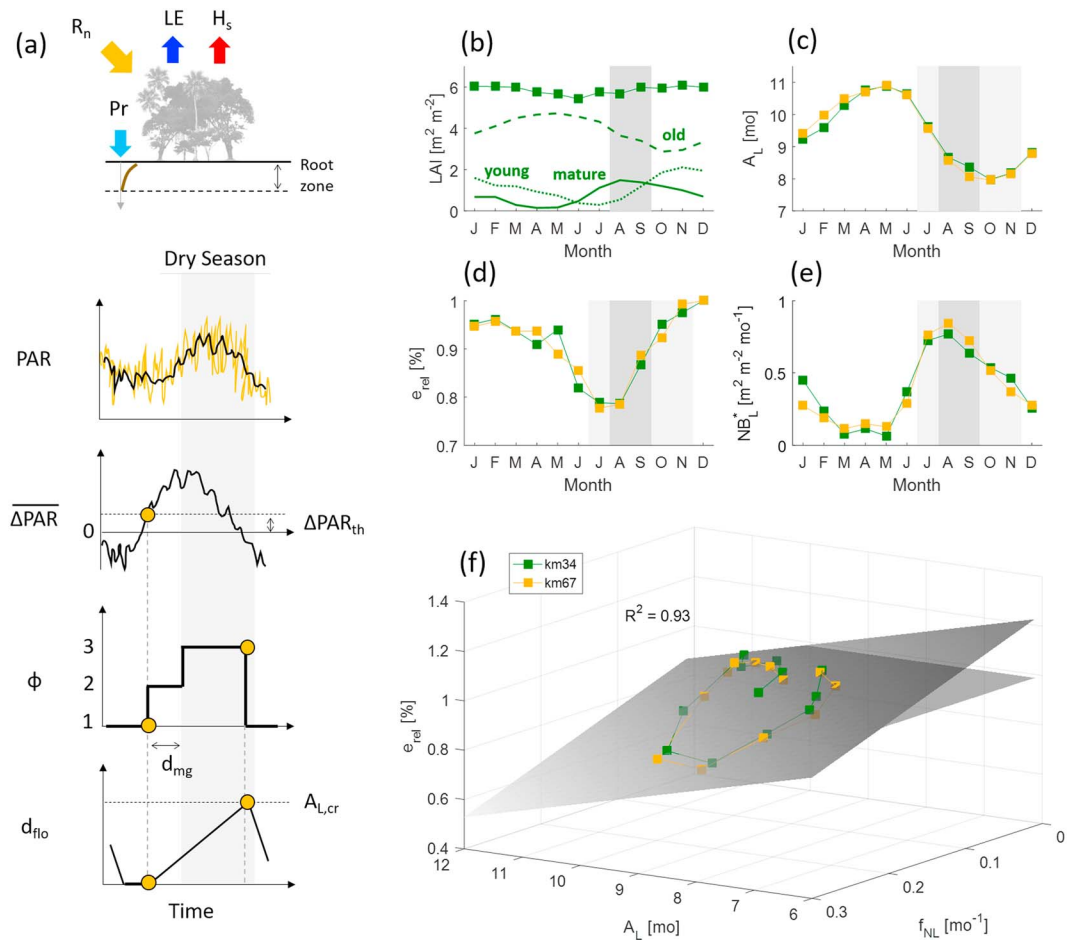


**Figure 1.** Conceptualization of the leaf phenology model developed for tropical rainforests (a), observations from sites km34 and km67 (b–e), and parameterization of  $e_{rel}$  (f). Data are digitized from Wu et al. (2016). Phenological states ( $\Phi$ ) and the count of days from the new season beginning ( $d_{flo}$ ) are regulated by changes in PAR ( $\Delta PAR$ ) exceeding an assigned threshold ( $\Delta PAR_{th}$ ). See main text for details on the calculation of  $\Delta PAR_{th}$ . (c) Canopy leaf age  $A_L$  [mo] is estimated using a simple mixing model (Wu et al., 2016) accounting for the partition of total LAI (squares in b) into young (dotted line), mature (solid line), and old (dashed line) leaves (b) and assuming average ages of 1.5, 6, and 12 months, respectively. Only data for km34 are shown in (b) as similar trends are observed at km67 (Wu et al., 2016). Photosynthetic efficiency ( $e_{rel}$ ) and new leaf biomass production ( $NB_L^*$ ) are illustrated in panels (d) and (e), respectively. The dry season (i.e., monthly precipitation <100 mm; Christoffersen et al., 2014) is denoted by gray shaded regions (dark gray for km34, light gray for km67 in panels (c), (d), and (e)). The observed dependence of  $e_{rel}$  on  $A_L$  and  $NB_L^*$  is shown in panel (f) together with the interpolating plane (equation (1)). Note that a limit  $e_{rel} \leq 1$  is imposed. Given that seasonal changes in LAI are limited, the fraction of new leaves  $f_{NL} = k_c \frac{NB_L^*}{LAI}$  follows the same trend illustrated in panel (e) for  $NB_L^*$ . LAI = leaf area index; PAR = photosynthetic active radiation.

(Fatichi & Ivanov, 2014; Fatichi et al., 2015; Fatichi, Leuzinger, et al., 2016; Manoli et al., 2018; Paschalis et al., 2015, 2016; Pappas et al., 2016) and is applied here in a revised form to the Amazon rainforests. Consistently with other DGVMs (Restrepo-Coupe et al., 2017), in the case of evergreen biomes the original formulation of T&C does not simulate a phenologic cycle of photosynthetic efficiency, which is maintained fixed throughout the year. A modified T&C version incorporating the phenology of tropical evergreen ecosystems (i.e., equation (1) is therefore introduced next. Direct simulation of SIF is also implemented in T&C according to Lee et al. (2015). Additional information on model equations are provided in the supporting information while a list of variables and abbreviations is provided in Table 2.

### 2.3.2. T&C With Leaf Phenology

To describe the observed seasonality of photosynthesis, three phenological states ( $\Phi$ ) are employed (Figure 1a): preparation to the new season ( $\Phi = 1$ ), initial growth ( $\Phi = 2$ , corresponding to the beginning of a new season), and normal growth ( $\Phi = 3$ ). This tropical phenology model describes a succession of periodic

**Table 2**  
Variables Used in the Tropical Phenology Module and Listed in the Text

Symbol	Description	Units
$A_L$	Leaf age	months (mo)
$A_{L,cr}$	Critical leaf age	days (d)
$A_n$	Net carbon assimilation	$\mu \text{ mol CO}_2 \text{ m}^{-2} \text{ s}^{-1}$
$C_L$	Leaf carbon pool	$\text{gC m}^{-2}$
$\overline{\Delta PAR}$	Smoothed PAR time derivative	$\text{W m}^{-2} \text{ d}^{-1}$
$\Delta PAR_{th}$	Threshold for $\overline{\Delta PAR}$	$\text{W m}^{-2} \text{ d}^{-1}$
$d_{flo}$	Phenological index counting the days after new season beginning	d
$d_L$	Turnover rate of leaves	$\text{d}^{-1}$
$d_{mg}$	phenological parameter (days of initial growth)	d
$e_{rel}$	Photosynthetic efficiency	—
ET	Evapotranspiration	$\text{mm d}^{-1}$
$f_L$	Carbon allocation fraction to leaves	—
$f'_L$	Preliminary carbon allocation fraction to leaves	—
$f_{NL}$	monthly fraction of young (<1 month) leaves	$\text{mo}^{-1}$
GPP	Gross primary productivity	$\text{gC m}^{-2} \text{ d}^{-1}$
$g_s$	Stomatal conductance	$\text{mol CO}_2 \text{ m}^{-2} \text{ s}^{-1}$
$k_c$	Correction factor	—
LAI	Leaf area index	$\text{m}^2_{leaf} \text{ m}^{-2}_{ground}$
$NB_L$	New leaf biomass production	$\text{gC m}^{-2} \text{ mo}^{-1}$
$NB^*_L$	New leaf production	$\text{m}^2 \text{ m}^{-2} \text{ mo}^{-1}$
$N_{LAI}$	New leaf area increment	$\text{m}^2 \text{ m}^{-1} \text{ d}^{-1}$
$\Phi$	Phenological state	—
$\Psi_L$	Predawn leaf water potential	MPa
PAR	Photosynthetic active radiation	$\text{W m}^{-2}$
PC	Photosynthetic capacity	$\text{mol}_{CO_2} \text{ mol}^{-1}_{photons}$
$PC_{max}$	Maximum photosynthetic capacity	$\text{mol}_{CO_2} \text{ mol}^{-1}_{photons}$
SIF	Solar-induced fluorescence	$\text{W m}^{-2} \text{ sr}^{-1} \mu\text{m}^{-1}$
$S_L$	Specific leaf area	$\text{m}^2 \text{ gC}^{-1}$
$V_{c,max25}$	Maximum Rubisco capacity at 25°C	$\mu \text{ mol CO}_2 \text{ m}^{-2} \text{ s}^{-1}$

plant life cycles similar to the stages adopted for temperate ecosystems (Arora & Boer, 2005; Fatichi, 2010) but is modified to consider the peculiarities of tropical biomes, that is, observed synchronization of new leaf growth and litterfall with sunlight during the dry season (Huete et al., 2006; Wu et al., 2016).

Given that dry-season greening closely tracks sunlight seasonality (Huete et al., 2006; Wu et al., 2016), changes in photosynthetic active radiation (PAR) are used as the driver of leaf development. A new season ( $\Phi = 1 \rightarrow 2$ ) is set to begin when  $\overline{\Delta PAR} > \Delta PAR_{th}$ , where  $\overline{\Delta PAR} = \langle \langle PAR(t) \rangle_{30} - \langle PAR(t) \rangle_{45} \rangle_{10}$  is a smoothed time derivative of PAR and  $\Delta PAR_{th}$  is a specific threshold. The smoothing procedure is employed to remove the daily and subdaily oscillations. This is achieved by computing the 10-day average of the difference between  $\langle PAR(t) \rangle_{30}$  and  $\langle PAR(t) \rangle_{45}$ , that is, PAR averages over 30 and 45 preceding days, respectively.  $\overline{\Delta PAR}$  is negative when PAR (on average) decreases with time, positive otherwise. This choice is guided by the hypothesis that vegetation “senses” the arrival of a new light-rich dry season by detecting an increase in sunlight availability (Wright & Van Schaik, 1994) and is in accordance with observations of maximum leaf production 1 to 2 months before the peak in PAR (Wu et al., 2016). Note that a similar mechanism based on light controls was used to explain observed synchronous flowering in the tropics (Borchert et al., 2005). The signal ( $\overline{\Delta PAR}$ ) is a non-instantaneous sunlight control on rainforest greening as the new season starts when the threshold  $\Delta PAR_{th}$  is reached. The threshold  $\Delta PAR_{th}$  is theoretically zero (i.e., the new season starts when  $\overline{\Delta PAR}$  switches from negative to positive) but values of 0.75–1 ( $\text{W m}^{-2} \text{ d}^{-1}$ ) are used here to account for the remaining noise

in  $\overline{\Delta PAR}$  (see Figure 1 and supporting information Figure S1). At the end of stage  $\Phi = 1$  and during  $\Phi = 2$  a large fraction of the assimilated carbon is allocated to new leaf biomass  $NB_L$  to support the observed light-controlled green-up.

The preliminary carbon allocation fraction to leaves is computed as  $f'_L = 1 - d_{fl_0}/A_{L,cr}$  where  $A_{L,cr}$  is the critical leaf age (d), which is a model parameter and  $d_{fl_0}$  [d] is a phenological index counting the days after the beginning of the new season and computed as  $d_{fl_0}(t + dt) = d_{fl_0}(t) + dt$ , with  $dt = 1$  day (see Figure 1a). The remaining assimilated carbon is partitioned among fine roots, living sapwood, carbohydrate reserves, and reproductive organs using functional allocation fractions and considering allometric constraints that define final allocation fractions as in the original T&C (Fatichi et al., 2012a, 2012b). Tropical evergreen forests do not experience proper senescence and dormant phases and carbon is allocated to reproductive organs year-round. The transition to the normal growth phase ( $\Phi = 2 \rightarrow 3$ ) takes place when  $d_{fl_0} > d_{mg}$ , where  $d_{mg}$  (d) is a prescribed number of days, while the transition  $\Phi = 3 \rightarrow 1$  occurs when  $d_{fl_0} > A_{L,cr}$ . The parameters  $A_{L,cr}$  and  $d_{mg}$  are employed in T&C also for other biomes and their values for tropical forests have been estimated, respectively, from observations and during model calibration (see next subsection). Even though allocation dynamics are variable throughout the year (Figure S1), from a modeling perspective phase  $\Phi = 1$  is identical to normal growth ( $\Phi = 3$ ) with the only difference that it allows for the preparation to a new season. The criterion used for the transition to  $\Phi = 1$  (i.e.,  $d_{fl_0} > A_{L,cr}$ ) ensures that the new season cannot start before the leaves produced in the previous year have reached maturity. During phase  $\Phi = 1$ ,  $d_{fl_0}$  is scaled back as  $d_{fl_0}(t + dt) = d_{fl_0}(t) - \frac{365}{365 - A_{L,cr}} dt$  to progressively increase allocation to new leaves and prepare for phase  $\Phi = 2$  (Figures 1 and S1).

To increase litterfall with leaf onset (Wu et al., 2016), the turnover rate of leaves  $d_L$  ( $d^{-1}$ ) is modified to include  $NB_L$  ( $gC\ m^{-2}\ d^{-1}$ ) as follows:

$$d_L(t) = \begin{cases} \frac{NB_L(t) \cdot A_{L,cr}}{C_L(t)} \cdot \frac{A_L(t)}{A_{L,cr}^2} & \text{if } NPP > 0 \\ \frac{A_L}{A_{L,cr}^2} & \text{if } NPP \leq 0 \end{cases} \quad (3)$$

where  $A_L$  [d] is the prognostic leaf age and  $C_L$  is the leaf carbon pool ( $gC\ m^{-2}$ ). Leaf age  $A_L$  is calculated as follows (Fatichi, 2010; Krinner et al., 2005):

$$A_L(t) = \frac{[LAI(t) - N_{LAI}(t)] \cdot [A_L(t - dt) + dt] + N_{LAI}(t)dt}{LAI(t)} \quad (4)$$

where  $N_{LAI}$  is the new leaf area increment [ $m^2\ m^{-2}$ ] on a time step and  $dt$  is the daily time step. For seasonal tropical evergreens, the turnover rate of leaves is assumed to be proportional to the ratio of newly produced leaves to the total biomass ( $\frac{NB_L(t)}{C_L(t)}$ ), thus generating faster turnover times during leaf production and mimicking the observed behavior of shedding old leaves to create space for new ones (Wu et al., 2016). For an aseasonal forest  $\frac{NB_L(t)}{C_L(t)} = \frac{1}{A_{L,cr}}$  and  $d_L$  becomes equal to the original T&C version without tropical phenology.

Equations (1)–(4) provide a novel mechanistic approach for the simulation of phenology-controlled seasonality in tropical evergreen forests. Compared to the original T&C formulation, the new approach introduces only one additional model parameter ( $\Delta PAR_{th}$ ).

### 2.3.3. Simulation Setup

To assess the impact of leaf phenology on carbon/water fluxes in the Amazon basin, both the original (T&C) and new (T&C with tropical phenology) model formulations are employed here. Meteorological forcings measured at the 32 study sites are used as model inputs. Partition of solar radiation into diffuse and direct components and in two wavebands is carried out by using the weather generator AWE-GEN (Fatichi et al., 2011). Model parameters are calibrated at one site (km67), and results are validated at three locations (km34, CAX, and RJA) for both model formulations with only few changes in the parameters set to tailor the application to site-specific characteristics (e.g., rooting depth, see Table S1). Based on literature values (e.g., Bahar et al., 2017; Baraloto et al., 2010), calibration was carried out by manually adjusting the most sensitive parameters for photosynthesis and transpiration (Mastrotheodoros et al., 2017). Calibrated parameters are then used to form two sets of average biome-specific parameters (one for each model version) and applied to the remaining 30 sites (Table S1). To be consistent with the theory of a common phenological mechanism operating across climatic

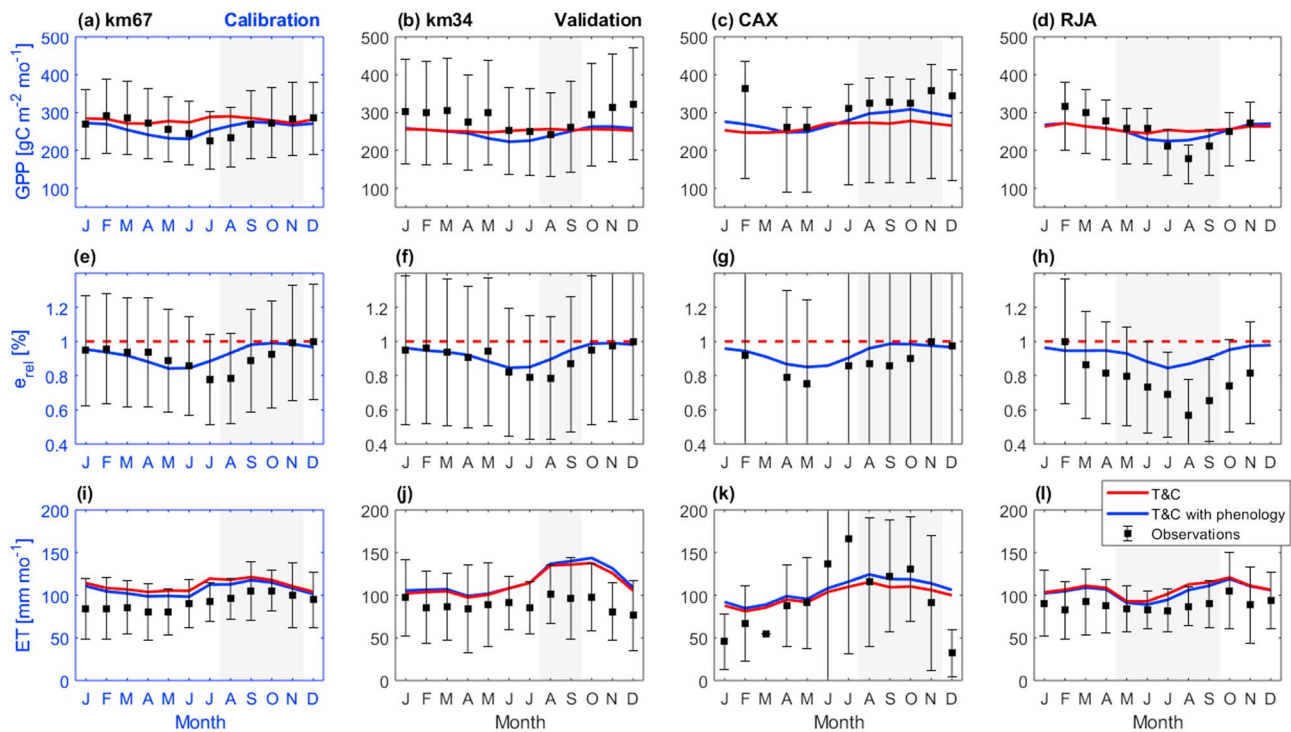


**Figure 2.** Observed and simulated GPP,  $e_{rel}$ , and ET for the calibration (km67) and validation (km34, CAX, and RJA) sites in the Amazon basin (blue and black boxes, respectively). Simulation results are shown for both the original and modified (i.e., with phenology) model formulations (red and blue lines, respectively). The dry season (i.e., monthly precipitation < 100 mm) is denoted by gray shaded regions. Error bars indicate  $\pm 1$  standard deviation. In the case of digitized data ( $e_{rel}$  and GPP), the standard deviation is estimated from the coefficient of variation of ET. ET = evapotranspiration; GPP = gross primary productivity.

gradients (Wu et al., 2016), physiological/phenological parameters are kept constant among sites and only climate drivers and soil properties are varied. Soil hydraulic parameters (saturated hydraulic conductivity and soil water retention curves) are estimated from soil textural properties (clay, sand, and organic matter content) obtained for the site or retrieved from the SoilGrids250m database (Hengl et al., 2017), using the pedotransfer functions by Saxton and Rawls (2006) with proper changes to account for tropical clay specificity (see the supporting information for details).

Changes in the generic flux or variable  $Y$  (i.e.,  $Y = \{GPP, ET, LAI\}$ ) due to leaf phenology ( $\Delta Y$  [%]) are then estimated as:

$$\Delta Y = \frac{Y_{T\&C \text{ with phenology}} - Y_{T\&C}}{Y_{T\&C}} \cdot 100 \quad (5)$$

where  $Y_{T\&C}$  and  $Y_{T\&C \text{ with phenology}}$  are the simulation results obtained with the original and modified T&C model versions, respectively.

The two model versions are run with a few different calibrated parameters and  $\Delta Y$  thus represents possible discrepancies due to tropical leaf phenology but also model parameters. To ensure that the calibration procedure does not confound the effects of leaf phenology, we run additional model simulations using a single set of calibrated parameters (see the supporting information for details). Results are very similar, suggesting that the introduction of phenology rather than small differences in parameters is the main source of difference between the two numerical experiments.

To ensure good quality of the meteorological forcing, only data from flux towers and meteorological stations are considered. A basin-wide analysis could be performed by using model-derived reanalysis data. However, the large bias in precipitation generally found in the tropics (e.g., Bosilovich et al., 2008) motivates our choice of a plot-scale multisite analysis rather than a distributed analysis with incorrect local climatic forcing.

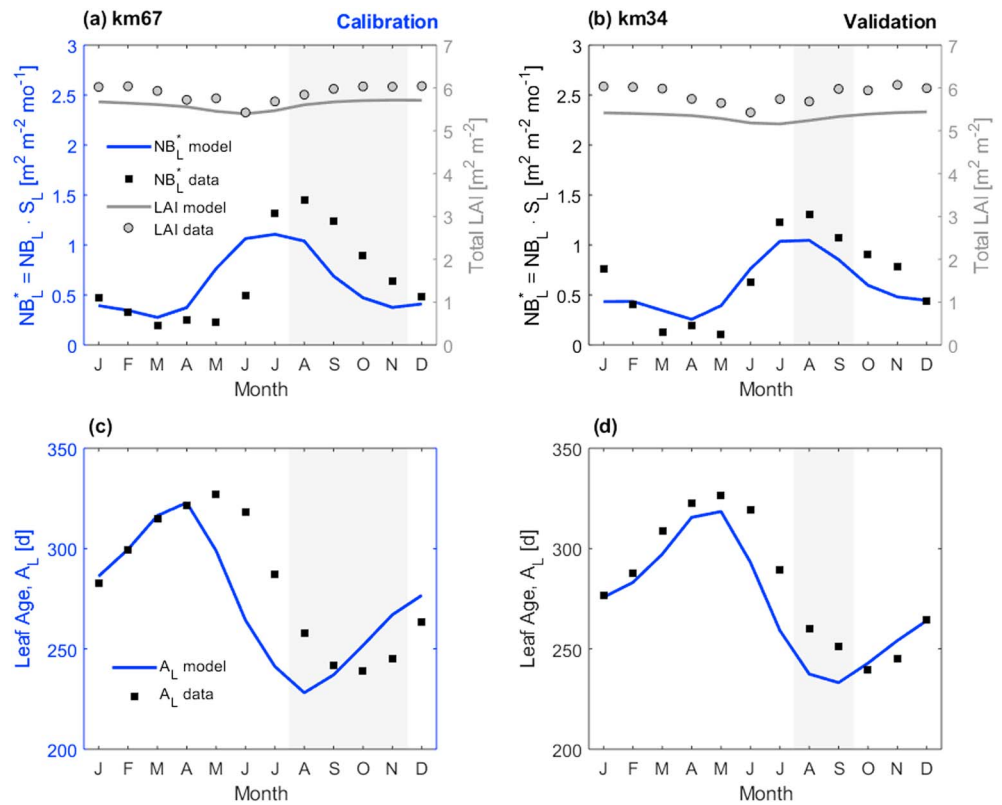


**Figure 3.** Observed and simulated LAI, new leaf production  $NB_L^* = NB_L \cdot S_L$ , that is, new leaf mass times specific leaf area (a and b), and leaf age  $A_L$  (c and d) at km34 and km67 sites. New leaf data ( $NB_L^*$ ) are digitized from Wu et al. (2016) and scaled by  $k_c$  to ensure consistency between LAI, litterfall, and leaf production (see main text for details). Simulation results are obtained using the modified model version (T&C with phenology). LAI = leaf area index; T&C = Thetys & Chloris.

### 3. Results

#### 3.1. Calibration and Validation

Calibration and validation results are illustrated in Figure 2. The original model version (without leaf phenology) assumes a fixed photosynthetic efficiency throughout the year ( $e_{rel} = 1$ ) and provides seasonal fluxes comparable with other DGVMs (see Restrepo-Coupe et al., 2017): The seasonality of ET fluxes is generally correct but the dry season increase in GPP is not captured. When leaf phenology is introduced, model simulations successfully reproduce PC seasonality and capture the observed dry-season greening. In particular, the correlation coefficient ( $r$ ) between modeled and observed hourly GPP increased from 0.20 and 0.41 to 0.34 and 0.52 for km67 and km34, respectively (see the supporting information). At monthly time scales and across the different sites,  $r$  increased from 0.2 to 0.5 (Figure S6). Note that the same set of parameters is used for all of the sites and, considering the uncertainties of flux tower observations in the tropics, the result can be considered to be a significant improvement. Interestingly, despite the changes in PC and GPP seasonality, simulated ET fluxes are only slightly affected by leaf phenology, thus preserving a good agreement with observations and reproducing coherently the seasonality of ET and GPP. This result is explained by the limited variability of LAI (Figure 3). While the production of new leaf biomass modifies mean leaf age (thus affecting the photosynthetic efficiency through  $e_{rel}$ ), the synchronization of leaf onset and litterfall limits LAI changes and, consequently, the impact on ET fluxes (see the supporting information). All these processes are well captured by the modified model version, T&C with phenology (Figures 3 and S1), which has only one additional parameter. Additional comparisons between observations and model results are illustrated in the supporting information for energy fluxes, GPP, and soil moisture dynamics.

#### 3.2. Multisite Analysis

Model simulations are then used to evaluate the seasonal and interannual variability of carbon and water fluxes in the Amazon. An overview of GPP, ET, and LAI as well as soil and predawn leaf water potential across

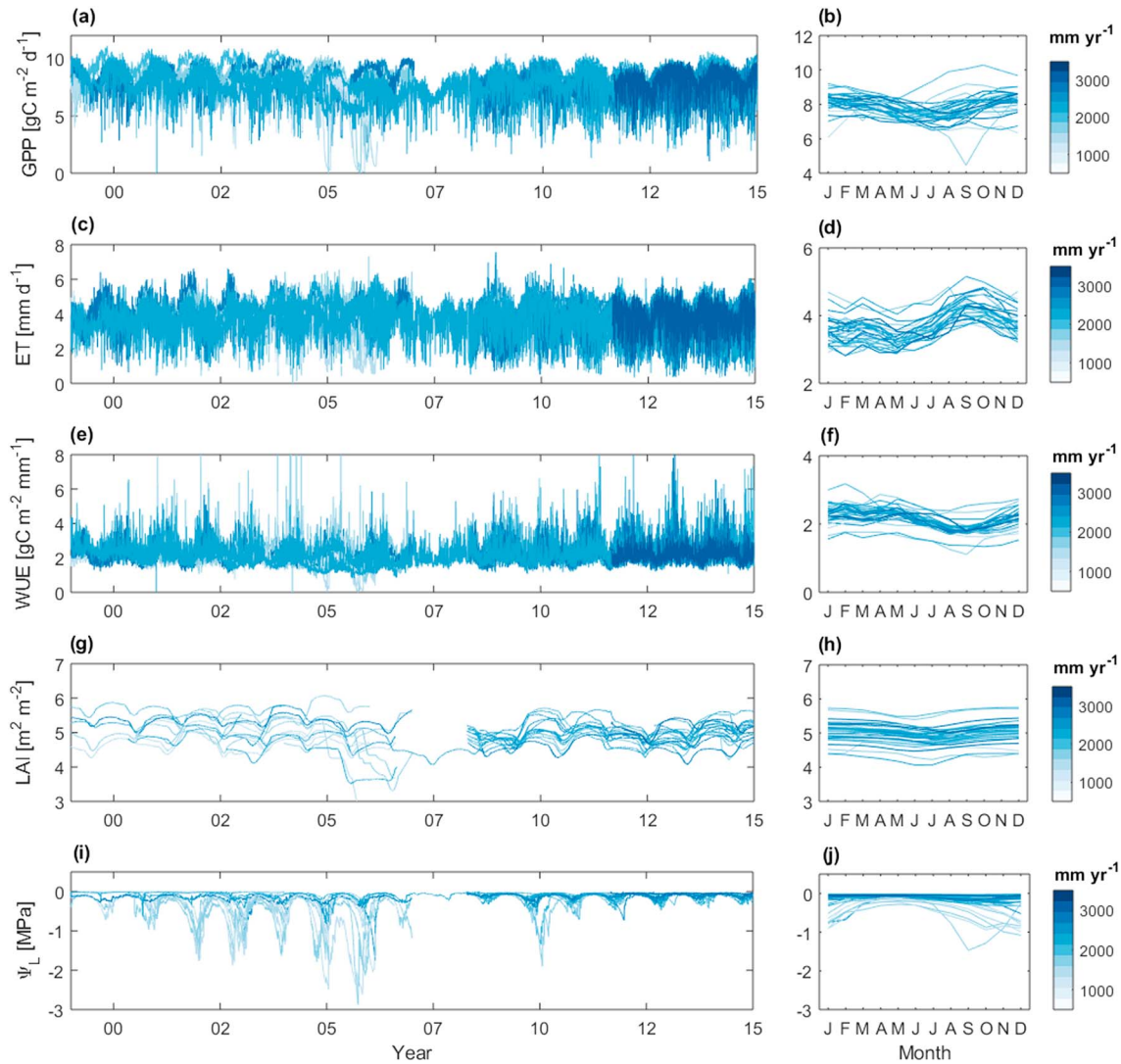


**Figure 4.** Daily simulated GPP (a and b), ET (c and d), WUE (e and f), LAI (g and h), and predawn leaf water potential  $\Psi_L$  (i and j) at the 34 study sites using the modified T&C model (T&C with phenology). Colors indicate the magnitude of mean annual precipitation, MAP (mm/year), at the different study sites. ET = evapotranspiration; GPP = gross primary productivity; LAI = leaf area index; T&C = Thetys & Chloris; WUE = water use efficiency.

the study sites from year 1999 to 2015 is provided in Figures 4 and 5. Note that different sites cover different periods of time. Also, predawn leaf water potential is a model quantity that integrates soil water potential over the root zone weighted to account for fine root vertical distribution and expresses an ecosystem-scale quantity that does not necessarily correspond to leaf-level observations of different species and thus should be interpreted with care.

GPP is shown to be lower at the beginning of the dry season and reach a maximum by the end of the dry season, with values generally ranging between 6 and 10  $\text{gC m}^{-2} \text{d}^{-1}$ . GPP dynamics are delayed compared to ET fluxes that increase early in the dry season ( $\text{ET} > 5 \text{ mm d}^{-1}$ ) and then decrease as the dry season progresses. However, monthly averages of forest ET never fall below 2  $\text{mm d}^{-1}$ . Model simulation show ET values larger than observations, but flux tower measurements are likely to considerably underestimate evaporation from ground and intercepted water, especially after precipitation (Gerken et al., 2017; Hirschi et al., 2017; Leuning et al., 2012). Overall, the dry season increase in GPP, timed with LAI and ET increments, is consistent across sites (Figures 4b, 4d, and 4h) but clear spatial patterns of GPP and ET with mean annual rainfall (MAP) are not observed (see next section). The water use efficiency  $\text{WUE} = \text{GPP}/\text{ET}$  ( $\text{gC m}^{-2} \text{mm}^{-1}$ ) is low at the end of the wet season and then increases during the dry months, indicating a more efficient water consumption linked to leaves with higher photosynthetic capacity as the ET demand increases.

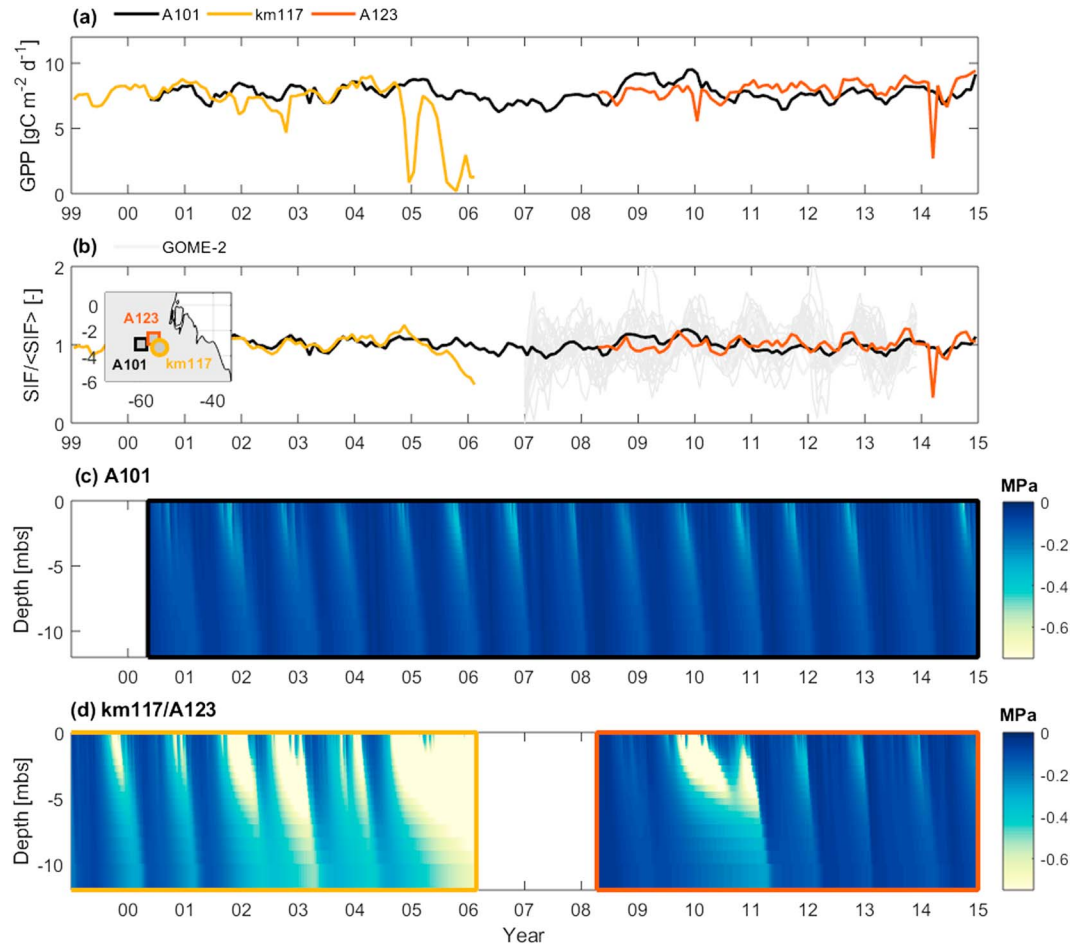


**Figure 5.** Simulated monthly averages of GPP (a), SIF (b), and soil water potential (c and d) at sites A101, km117, and A123. SIF observations from GOME-2 (Joiner et al., 2013) at the 32 sites are also illustrated for a qualitative comparison (grey lines in panel b). The inset in panel b shows the location of the selected study sites. GOME-2 = Global Ozone Monitoring Instrument 2; GPP = gross primary productivity; SIF = solar-induced fluorescence.

Plant water stress (Figure 4j) can occur at end of the dry season causing a reduction in ET, but ET is generally modulated by incoming radiation. Model simulations clearly illustrate that several sites likely have experienced water stress with major drought events in 2005 and 2010 (Liu et al., 2018). However, leaf water potential is close to zero (i.e., no water stress) for most places most of the time and only major droughts are evident with simulated predawn leaf water potential  $\Psi_L < -1$  MPa at several locations (Figure 4i). Our results suggest that the 2010 drought was an “independent” severe event, while plant water stress in 2005 was the result of successive dry seasons that exacerbated drought through legacy effects. These results are consistent with the observed increase in tree mortality during the 2005 drought event (Meir et al., 2009; Phillips et al., 2009) and the greater anomalies in vegetation water content recorded in 2005 compared to 2010 (Liu et al., 2018) but, given the difficulties in comparing modeled  $\Psi_L$  with observations and the paucity of  $\Psi_L$  measurements, results cannot be rigorously confirmed.

The decrease in LAI at the end of the wet season (Figures 3 and 4h) reduces ET thus saving soil water for the upcoming dry months, but the impact on the magnitude of ET is minimal. LAI dynamics show little seasonality, the variability across sites is higher than seasonal variations, and LAI values range between 4 and 5.5  $\text{m}^2 \text{m}^{-2}$ . The dry season increase in LAI and GPP (i.e., greening during August–November) is clearly reproduced in Figure 5, where simulated and observed SIFs are also illustrated for comparison. During the 2005 drought, some sites (e.g., A101) show no water stress and a dry season increase in GPP, while other locations (e.g., km117) experience severe stress with a substantial decrease in productivity and, potentially, forest mortality (Phillips et al., 2009). Even though fewer locations across the study sites seem to have experienced stress

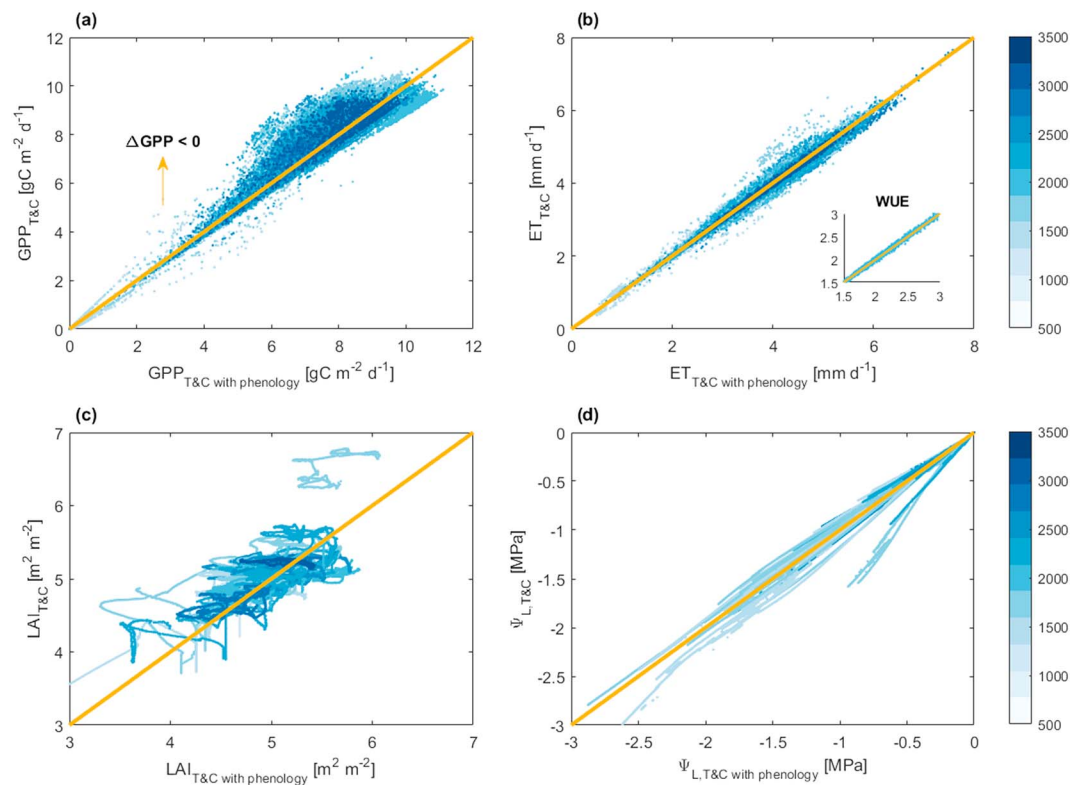


**Figure 6.** Comparison of simulation results (daily values) with and without leaf phenology: GPP (a), ET (b), LAI (c), and predawn leaf water potential  $\psi_L$  (d). Water use efficiency ( $WUE = GPP/ET$  [ $gC\ m^{-2}\ mm^{-1}$ ]) is also shown (inset in panel b). Colors indicate mean annual precipitation values, MAP (mm/year), at the different study sites. The 1:1 line is illustrated for comparison (yellow line). ET = evapotranspiration; GPP = gross primary productivity; LAI = leaf area index.

in 2010, the severity of drought in some locations is clearly illustrated by the temporal evolution of the soil water potential (Figure 5d), which caused a sharp GPP reduction (see sites km117 and A123).

### 3.3. The Role of Leaf Phenology

The impact of leaf phenology on water/carbon fluxes is now evaluated by comparing simulation results from the original and modified model versions (T&C and T&C with tropical phenology, respectively). Hourly values of GPP, ET, LAI, and  $\Psi_L$  simulated with and without leaf phenology are illustrated in Figure 6. When phenology is neglected, model results generally overestimate the total carbon uptake ( $\Delta GPP < 0$ ) as the GPP reduction before the dry season is not captured (see Figures 2 and 6a and Restrepo-Coupe et al., 2017). As expected little variations are observed in the ET fluxes and, given the changes on both GPP and ET, no appreciable deviations in WUE are simulated (Figure 6b). Negative LAI changes ( $\Delta LAI$ ) are also obtained (Figure 6c), but they are relatively small ( $< 1\ m^2\ m^{-2}$ ), and, at each site, LAI oscillates within a small range of values (Myneni et al., 2007). Overall, the onset of new leaves at the beginning of the dry season can potentially increase forest resilience to drought (i.e., its ability to maintain unaltered carbon and water fluxes under extremely dry conditions) by maintaining more favorable leaf water potentials during drought (Figure 6d) and sustain water fluxes during the dry season. This mechanism is explained by a decrease in LAI at the end of the wet season that reduces ET, maintain favorable soil water conditions, and sustain ET maxima during the dry season (Wu et al., 2016). However, our results suggest that such a phenology-induced increase in forest resilience should be relatively limited and additional field measurements are required to test this assertion and support it with more quantitative evidence. Note that model simulations with and without phenology are run considering different sets of calibrated parameters but calibration was tested to have a negligible effect on the phenology-induced changes observed in Figure 6 (see the supporting information).

The spatial distribution of carbon/water fluxes and phenology-induced changes in GPP, ET, and LAI is illustrated in Figure 7. On average (yearly and among sites), the addition of leaf phenology results in GPP, ET,

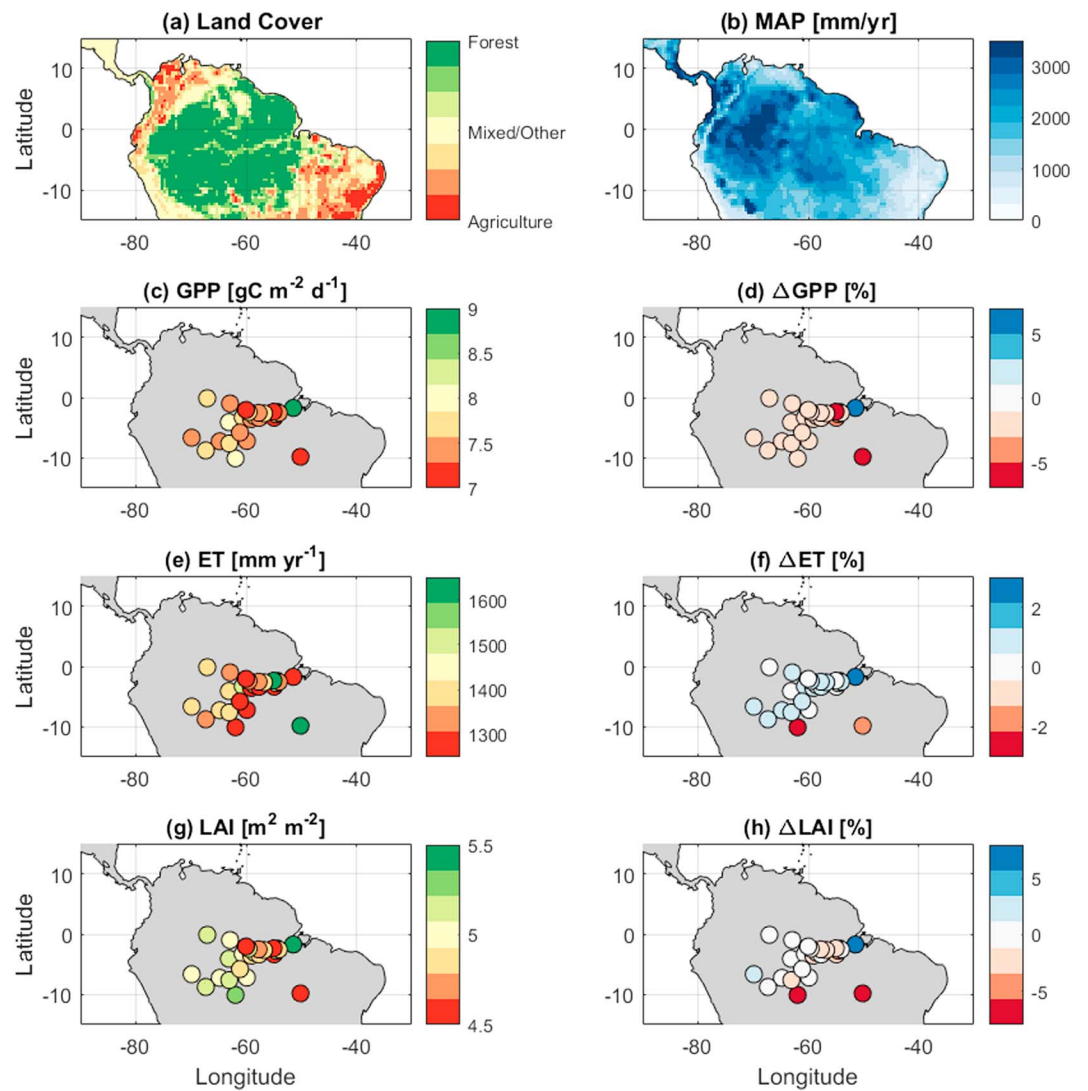


**Figure 7.** Land cover (a) and mean annual precipitation (MAP) (b) in tropical Amazonia. Simulated GPP, ET, and LAI (mean annual values) at the 34 study sites using T&C with phenology are illustrated in panels c, e, and g. Phenology-induced changes in simulated GPP, ET, and LAI are shown in panels d, f, and h. Land cover data are derived from the Global Land Cover 2000 database (European Commission, Joint Research Centre, 2003), while precipitation is based on the GPCP Full Data Reanalysis of monthly global land-surface precipitation (Schneider et al., 2015). ET = evapotranspiration; GPP = gross primary productivity; LAI = leaf area index; T&C = Thetys & Chloris.

and LAI changes of  $-2.56\%$ ,  $+0.4\%$ , and  $-1.3\%$ , respectively (with  $\Delta GPP \in [-7.6; 5.9]$ ,  $\Delta ET \in [-4.1; 5.9]$ , and  $\Delta LAI \in [-14.0; 10.8]$ ). While GPP is consistently overestimated when leaf phenology is neglected, changes in ET and LAI are small and no clear spatial pattern can be identified.

## 4. Discussion

### 4.1. Leaf Phenology in DGVMs

Global estimates of GPP are still highly uncertain (Badgley et al., 2017), and tropical carbon fluxes are poorly resolved in existing DGVMs (Restrepo-Coupe et al., 2017). Tropical forest GPP is a major component of the global carbon cycle (Musavi et al., 2017), and understanding its seasonal and interannual variability is crucial to predict global climate dynamics. Here we have provided a novel mechanistic approach to represent leaf phenology and GPP seasonality that requires a single parameter and is general enough to be used in any DGVM that has a prognostic phenology and simulates leaf age. Its inclusion can improve the assessment of carbon and water fluxes in the tropics. We have shown that carbon uptake is likely to be biased by current DGVMs simulations and, in the absence of leaf phenology, model parameterization can lead to both

an underestimation and overestimation of photosynthesis (as happened here, Figures 2a–2d). Previous efforts to include tropical phenology in DGVMs focused on parameterizing  $V_{c,max}$  as a function of leaf age (De Weirdt et al., 2012; Kim et al., 2012) and introducing a radiation-dependent leaf turnover rate (Kim et al., 2012). These modifications improved the ability of models to capture the seasonality of litterfall (De Weirdt et al., 2012) and carbon fluxes (Kim et al., 2012). Here we introduced a mechanistic link between light controls, leaf demography, and photosynthetic efficiency and we have shed light on seasonal dynamics of forest ET and ecosystem responses to drought. This approach is consistent with recent field observations showing that mature leaves have “better quality” (i.e., higher  $V_{c,max}$ ) than young and old leaves and their quantity increases during the dry season (Albert et al., 2018; Wu et al., 2016). Building on this knowledge, future model improvements could focus on the explicit representation of different leaf age classes that are encoded here in a single canopy age,  $A_L$ , and another variable, which is the fraction of young leaves  $f_{NL}$ . Such a modification might improve the timing of simulated leaf flush (Figure 3) and allow a direct comparison with available data for young, mature, and old leaves (Albert et al., 2018). In this regard, more resolved litterfall and biomass production data as well as observations from more locations in the tropics are needed to better assess the performance of tropical phenology schemes.

#### 4.2. Leaf Phenology and Water Stress in the Amazon Rainforest

Coordinated ecosystem-scale phenology is likely to be an evolutionary strategy to maximize photosynthesis during drier but light-richer periods (Myneni et al., 2007) and optimize carbon gain in year-round warm climates (Wu et al., 2016). On evolutionary timescales, producing leaves and flowers in synchronous flushes during the dry season could also be an “escape” strategy to reduce the damages from herbivores, which are more abundant at the beginning of the wet season (Aide, 1988, 1992) or the result of biotic interactions between plants and pollinators (Borchert et al., 2005). However, these responses to biotic pressures are largely neglected in the context of DGVMs, and seasonal variations in rainfall, light, and soil water availability are generally accepted as the major causes of observed tropical phenology (Borchert et al., 2004; Brando et al., 2006; Kim et al., 2012; Wright & Van Schaik, 1994; Wu et al., 2016). Our results confirm the hypothesis that leaf phenology may act to facilitate dry season maxima in water fluxes (Chavana-Bryant et al., 2016; Wu et al., 2016) since we found little evidence of soil moisture stress in most of the locations with ET fluxes supported by deep root water uptake. Existing evidence suggests that such late dry season fluxes are key to activating shallow convection and initiate the dry-to-wet season transition (Machado et al., 2004; Wright et al., 2017). In this framework leaf phenology can help enhance resilience to drought by reducing LAI at the end of the wet season, thus “saving” soil water for the upcoming dry months but quantitative evidence is minimal. The impact on ET is relatively small (+0.4%), indicating that tropical leaf phenology may have little impact on forest tolerance to drought, and implications for simulated rainfall recycling (Betts et al., 2004; Bonetti et al., 2015; Eltahir & Bras, 1994) and climate teleconnections (Stark et al., 2016; Wright et al., 2017; Wu et al., 2016) should be limited. However, the simulated seasonality of WUE suggest that leaf development and synchronized dry season litterfall are in agreement with evolutionary strategies aimed at increasing the efficiency of photosynthesis and water consumption during periods of abundant light but potentially low water availability (i.e., at the end of the dry season).

The small sensitivity of ET to leaf phenology is explained by the fact that changes in the maximum Rubisco capacity ( $V_{c,max25}^*$ ) due to seasonality (i.e.,  $e_{rel}$ ) have direct effects on carbon assimilation ( $A_n$ ) and GPP according to the Farquhar model  $A_n$  is proportional to  $V_{c,max25}^*$  in light-rich environments; Bonan et al., 2011; Collatz et al., 1991; Farquhar et al., 1980; see the supporting information) but only an indirect impact on ET through changes in the stomatal conductance ( $g_s$ ) of sunlit and shaded leaves (modeled according to Leuning, 1995, in T&C). In particular, while  $e_{rel}$  affects  $g_s$ , the impact of leaf phenology on transpiration is buffered by canopy-atmosphere decoupling (De Kauwe et al., 2017), significant for tall broadleaf tropical forests, and concomitant LAI changes, which reduce the changes in ET as compared to  $\Delta GPP$  (see the supporting information for details).

Our results also show that Amazonian forests experienced a severe water stress in 2005 due to a legacy effect of deficient rainfall in previous dry/wet seasons that aggravated water stress by systematically decreasing soil-plant water potentials (Figure 4i). Such legacy effects were not visible in 2010, probably due to a very wet 2009 (Marengo et al., 2011). Thus, the hypothesis that tropical forest are resilient to short-term climatic anomalies (Saleska et al., 2007) but vulnerable to prolonged (i.e., multiyear) drought events (Nepstad et al., 2007; Ivanov et al., 2012) is generally supported here. Furthermore, these results are consistent with the observations of severe drought events in the Amazon region in 2005 and 2010 (Lewis et al., 2011; Marengo et al., 2011).

After the 2005 drought an increase in tree mortality was observed (Phillips et al., 2009) and a suppression of photosynthesis caused a neutralization of the carbon sink in 2010 (Gatti et al., 2014). A multisite analysis by Doughty et al. (2015) also revealed that trees' allocation to maintenance and defence tissues decreased during the 2010 drought, thus increasing the risk of postdrought mortality.

Basin-wide drought assessments based on satellite-derived rainfall data have considerable uncertainty as compared to plot-scale analyses that are also better representing effects of local soil conditions and soil-moisture temporal and vertical variability. As a matter of fact, ecosystem functioning and productivity are directly linked to soil water availability rather than rainfall (Bonetti et al., 2017; Fatichi, Pappas, et al., 2016). Hence, despite the spatial limitation of our analysis (performed at the plot-scale in multiple sites), the simulation of coupled soil-plant-atmosphere processes here provides an insightful quantification of the mechanisms regulating dry-season greening and water stress in the Amazon. In particular, we show that depending on complex interactions between rainfall variability, soil water content, and canopy phenological state, plot-scale forest productivity can both increase or decrease during the dry season (see simulated GPP in 2005 and 2010; Figure 5). These results are consistent with the observed heterogeneities of basin-wide responses to drought reported in the literature (Lewis et al., 2011; Phillips et al., 2009).

## 5. Conclusions

A novel approach to model GPP seasonality in the tropics and a multisite, multiyear analysis relying on locally observed meteorological data only and illustrating forest responses to climate variability across the Amazon basin over a 15-year period has been presented. Our results provide a first mechanistic description of tropical leaf phenology, reconciling observed dry-season greening and water limitations in the Amazon and paving the way for future model analyses accounting for photosynthetic seasonality in the tropics. Leaf phenology is shown to influence considerably ecosystem carbon fluxes with little impact on evapotranspiration and resilience to short-term drought. Phenology-related inaccuracies in the simulation of water and energy fluxes are unlikely, but existing DGVMs generally overestimate or underestimate GPP, because they lack a seasonal cycle of photosynthetic efficiency. Accounting for the effects of leaf quality and quantity on photosynthesis is therefore crucial to accurately describe the Amazon carbon balance from hourly to decadal timescales.

## Acknowledgments

This study was supported by the Swiss National Science Foundation (r4d-Ecosystems, n. 152019). G. Manoli acknowledges support by the U.S. National Science Foundation (NSF-EAR-1344703), and V. Ivanov was supported by the DOE OBER grant DE-SC0011078 Understanding the Response of Photosynthetic Metabolism in Tropical Forests to Seasonal Climate Variations ("GoAmazon"). The authors would like to thank João Verde and the Instituto Nacional de Meteorologia-Ministério da Agricultura, Pecunária e Abastecimento, Brasil, for providing the INMET data; Federica Remondi and Nadav Peleg for help in the preparation of model inputs; and Bradley Christoffersen for help and discussions at the beginning of this research. We also thank the associate editor and two anonymous reviewers for the constructive comments. The authors confirm that they have no interest or relationship, financial, or otherwise that might be perceived as influencing objectivity with respect to this work. The data used are listed in the references, tables, and supporting information.

## References

- Ahlström, A., Canadell, J. G., Schurgers, G., Wu, M., Berry, J. A., Guan, K., & Jackson, R. B. (2017). Hydrologic resilience and Amazon productivity. *Nature Communications*, 8, 387.
- Aide, T. M. (1988). Herbivory as a selective agent on the timing of leaf production in a tropical understory community. *Nature*, 336(6199), 574–575.
- Aide, T. M. (1992). Dry season leaf production: an escape from herbivory. *Biotropica*, 24, 532–537.
- Albert, L. P., Wu, J., Prohaska, N., Camargo, P. B., Huxman, T. E., Tribuzy, E. S., et al. (2018). Age-dependent leaf physiology and consequences for crown-scale carbon uptake during the dry season in an Amazon evergreen forest. *New Phytologist*. <https://doi.org/10.1111/nph.15056>
- Alden, C. B., Miller, J. B., Gatti, L. V., Gloor, M. M., Guan, K., Michalak, A. M., et al. (2016). Regional atmospheric CO<sub>2</sub> inversion reveals seasonal and geographic differences in Amazon net biome exchange. *Global Change Biology*, 22(10), 3427–3443.
- Arora, V. K., & Boer, G. J. (2005). A parameterization of leaf phenology for the terrestrial ecosystem component of climate models. *Global Change Biology*, 11(1), 39–59.
- Badgley, G., Field, C. B., & Berry, J. A. (2017). Canopy near-infrared reflectance and terrestrial photosynthesis. *Science Advances*, 3(3), e1602244.
- Bahar, N. H., Ishida, F. Y., Weerasinghe, L. K., Guerrieri, R., O'Sullivan, O. S., Bloomfield, K. J., et al. (2017). Leaf-level photosynthetic capacity in lowland Amazonian and high-elevation andean tropical moist forests of Peru. *New Phytologist*, 214(3), 1002–1018.
- Baker, I., Prihodko, L., Denning, A., Goulden, M., Miller, S., & Da Rocha, H. (2008). Seasonal drought stress in the Amazon: Reconciling models and observations. *Journal of Geophysical Research*, 113, G00B01. <https://doi.org/10.1029/2007JG000644>
- Baraloto, C., Timothy Paine, C., Poorter, L., Beauchene, J., Bonal, D., Domenach, A.-M., et al. (2010). Decoupled leaf and stem economics in rain forest trees. *Ecology Letters*, 13(11), 1338–1347.
- Betts, R., Cox, P., Collins, M., Harris, P., Huntingford, C., & Jones, C. (2004). The role of ecosystem-atmosphere interactions in simulated amazonian precipitation decrease and forest dieback under global climate warming. *Theoretical and Applied Climatology*, 78(1), 157–175.
- Boisier, J. P., Ciais, P., Ducharne, A., & Guimberteau, M. (2015). Projected strengthening of Amazonian dry season by constrained climate model simulations. *Nature Climate Change*, 5(7), 656–660.
- Bonan, G. B., Lawrence, P. J., Oleson, K. W., Levis, S., Jung, M., Reichstein, M., et al. (2011). Improving canopy processes in the community land model version 4 (clm4) using global flux fields empirically inferred from fluxnet data. *Journal of Geophysical Research*, 116, G02014. <https://doi.org/10.1029/2010JG001593>
- Bonetti, S., Feng, X., & Porporato, A. (2017). *Ecophysiological controls on plant diversity in tropical south america* (Vol. 10, pp. e1853).
- Bonetti, S., Manoli, G., Domec, J.-C., Putti, M., Marani, M., & Katul, G. G. (2015). The influence of water table depth and the free atmospheric state on convective rainfall predisposition. *Water Resources Research*, 51, 2283–2297. <https://doi.org/10.1002/2014WR016431>
- Borchert, R. (1998). Responses of tropical trees to rainfall seasonality and its long-term changes.
- Borchert, R., Meyer, S. A., Felger, R. S., & Porter-Bolland, L. (2004). Environmental control of flowering periodicity in Costa Rican and Mexican tropical dry forests. *Global Ecology and Biogeography*, 13(5), 409–425.

- Borchert, R., Renner, S. S., Calle, Z., Navarrete, D., Tye, A., Gautier, L., et al. (2005). Photoperiodic induction of synchronous flowering near the equator. *Nature*, *433*(7026), 627–629.
- Bosilovich, M. G., Chen, J., Robertson, F. R., & Adler, R. F. (2008). Evaluation of global precipitation in reanalyses. *Journal of Applied Meteorology and Climatology*, *47*(9), 2279–2299.
- Brando, P. M., Goetz, S. J., Baccini, A., Nepstad, D. C., Beck, P. S., & Christman, M. C. (2010). Seasonal and interannual variability of climate and vegetation indices across the Amazon. *Proceedings of the National Academy of Sciences of the United States of America*, *107*(33), 14,685–14,690.
- Brando, P., Ray, D., Nepstad, D., Cardinot, G., Curran, L. M., & Oliveira, R. (2006). Effects of partial throughfall exclusion on the phenology of *Coussarea racemosa* (Rubiaceae) in an east-central Amazon rainforest. *Oecologia*, *150*(2), 181–189.
- Chavana-Bryant, C., Malhi, Y., Wu, J., Asner, G. P., Anastasiou, A., Enquist, B. J., et al. (2016). Leaf aging of Amazonian canopy trees as revealed by spectral and physiochemical measurements. *New Phytologist*, *214*(3), 1049–1063.
- Christoffersen, B. O., Restrepo-Coupe, N., Arain, M. A., Baker, I. T., Cestaro, B. P., Ciais, P., et al. (2014). Mechanisms of water supply and vegetation demand govern the seasonality and magnitude of evapotranspiration in Amazonia and Cerrado. *Agricultural and Forest Meteorology*, *191*, 33–50.
- Collatz, G. J., Ball, J. T., Grivet, C., & Berry, J. A. (1991). Physiological and environmental regulation of stomatal conductance, photosynthesis and transpiration: A model that includes a laminar boundary layer. *Agricultural and Forest Meteorology*, *54*(2–4), 107–136.
- Cox, P. M., Betts, R. A., Jones, C. D., Spall, S. A., & Totterdell, I. J. (2000). Acceleration of global warming due to carbon-cycle feedbacks in a coupled climate model. *Nature*, *408*(6809), 184–187.
- da Costa, A. C. L., Galbraith, D., Almeida, S., Portela, B. T. T., da Costa, M., de Athaydes Silva Junior, J., et al. (2010). Effect of 7 yr of experimental drought on vegetation dynamics and biomass storage of an eastern Amazonian rainforest. *New Phytologist*, *187*(3), 579–591.
- Davidson, E. A., de Araújo, A. C., Artaxo, P., Balch, J. K., Brown, I. F., Bustamante, M. M., et al. (2012). The Amazon basin in transition. *Nature*, *481*(7381), 321–328.
- De Gonçalves, L. G. G., Borak, J. S., Costa, M. H., Saleska, S. R., Baker, I., Restrepo-Coupe, N., et al. (2013). Overview of the large-scale biosphere–atmosphere experiment in Amazonia data model intercomparison project (LBA-DMIP). *Agricultural and Forest Meteorology*, *182*, 111–127.
- De Kauwe, M. G., Medlyn, B. E., Knauer, J., & Williams, C. A. (2017). Ideas and perspectives: How coupled is the vegetation to the boundary layer? *Biogeosciences Discussions*, *14*, 4435–4453.
- De Weirdt, M., Verbeeck, H., Maignan, F., Peylin, P., Poulter, B., Bonal, D., et al. (2012). Seasonal leaf dynamics for tropical evergreen forests in a process-based global ecosystem model. *Geoscientific Model Development*, *5*(5), 1091–1108.
- Doughty, C. E., Metcalfe, D., Girardin, C., Amézquita, F. F., Cabrera, D. G., Huasco, W. H., et al. (2015). Drought impact on forest carbon dynamics and fluxes in Amazonia. *Nature*, *519*(7541), 78–82.
- Eltahir, E. A., & Bras, R. L. (1994). Precipitation recycling in the Amazon basin. *Quarterly Journal of the Royal Meteorological Society*, *120*(518), 861–880.
- Farquhar, G., von Caemmerer, S., & Berry, J. (1980). A biochemical model of photosynthetic CO<sub>2</sub> assimilation in leaves of C<sub>3</sub> species. *Planta*, *149*(1), 78–90.
- Fatichi, S. (2010). The modeling of hydrological cycle and its interaction with vegetation in the framework of climate change (PhD thesis). University of Florence, University Braunschweig, Braunschweig, Germany.
- Fatichi, S., & Ivanov, V. Y. (2014). Interannual variability of evapotranspiration and vegetation productivity. *Water Resources Research*, *50*(4), 3275–3294.
- Fatichi, S., Ivanov, V. Y., & Caporali, E. (2011). Simulation of future climate scenarios with a weather generator. *Advances in Water Resources*, *34*(4), 448–467.
- Fatichi, S., Ivanov, V., & Caporali, E. (2012a). A mechanistic ecohydrological model to investigate complex interactions in cold and warm water-controlled environments: 1. theoretical framework and plot-scale analysis. *Journal of Advances in Modeling Earth Systems*, *4*, M05002. <https://doi.org/10.1029/2011MS000086>
- Fatichi, S., Ivanov, V., & Caporali, E. (2012b). A mechanistic ecohydrological model to investigate complex interactions in cold and warm water-controlled environments: 2. Spatiotemporal analyses. *Journal of Advances in Modeling Earth Systems*, *4*, M05003. <https://doi.org/10.1029/2011MS000087>
- Fatichi, S., Katul, G. G., Ivanov, V. Y., Pappas, C., Paschalis, A., Consolo, A., et al. (2015). Abiotic and biotic controls of soil moisture spatiotemporal variability and the occurrence of hysteresis. *Water Resources Research*, *51*(5), 3505–3524.
- Fatichi, S., Leuzinger, S., & Körner, C. (2014). Moving beyond photosynthesis: From carbon source to sink-driven vegetation modeling. *New Phytologist*, *201*(4), 1086–1095.
- Fatichi, S., Leuzinger, S., Paschalis, A., Langley, J. A., Barraclough, A. D., & Hovenden, M. J. (2016). Partitioning direct and indirect effects reveals the response of water-limited ecosystems to elevated CO<sub>2</sub>. *Proceedings of the National Academy of Sciences of the United States of America*, *113*(45), 12,757–12,762.
- Fatichi, S., Pappas, C., & Ivanov, V. Y. (2016). Modeling plant–water interactions: An ecohydrological overview from the cell to the global scale. *WIREs Water*, *3*(3), 327–368. <https://doi.org/10.1002/wat2.1125>
- Fitzjarrald, D. R., Sakai, R. K., Moraes, O. L., Cosme de Oliveira, R., Acevedo, O. C., Czikowsky, M. J., & Beldini, T. (2008). Spatial and temporal rainfall variability near the Amazon-Tapajós confluence. *Journal of Geophysical Research*, *113*, G00B11. <https://doi.org/10.1029/2007JG000596>
- Fu, R., Yin, L., Li, W., Arias, P. A., Dickinson, R. E., Huang, L., et al. (2013). Increased dry-season length over southern Amazonia in recent decades and its implication for future climate projection. *Proceedings of the National Academy of Sciences of the United States of America*, *110*(45), 18,110–18,115.
- Galbraith, D., Levy, P. E., Sitch, S., Huntingford, C., Cox, P., Williams, M., & Meir, P. (2010). Multiple mechanisms of Amazonian forest biomass losses in three dynamic global vegetation models under climate change. *New Phytologist*, *187*(3), 647–665.
- Gatti, L., Gloor, M., Miller, J., Doughty, C., Malhi, Y., Domingues, L., et al. (2014). Drought sensitivity of Amazonian carbon balance revealed by atmospheric measurements. *Nature*, *506*(7486), 76–80.
- Gerken, T., Ruddell, B. L., Fuentes, J. D., Araújo, A., Brunsell, N. A., Maia, J., et al. (2017). Investigating the mechanisms responsible for the lack of surface energy balance closure in a central Amazonian tropical rainforest. *Agricultural and Forest Meteorology*, *255*, 92–103.
- Guan, K., Pan, M., Li, H., Wolf, A., Wu, J., Medvigy, D., et al. (2015). Photosynthetic seasonality of global tropical forests constrained by hydroclimate. *Nature Geoscience*, *8*(4), 284–289.
- Hayek, M. N., Longo, M., Wu, J., Smith, M. N., Restrepo-Coupe, N., Tapajós, R., et al. (2018). Carbon exchange in an Amazon forest: from hours to years. *Biogeosciences Discussions*, *2018*, 1–26. <https://doi.org/10.5194/bg-2018-131>

- Hengl, T., de Jesus, J. M., Heuvelink, G. B., Gonzalez, M. R., Kilibarda, M., Blagotić, A., et al. (2017). Soilgrids250m: Global gridded soil information based on machine learning. *PLoS One*, *12*(2), e0169748.
- Hirschi, M., Michel, D., Lehner, I., & Seneviratne, S. I. (2017). A site-level comparison of lysimeter and eddy covariance flux measurements of evapotranspiration. *Hydrology and Earth System Sciences*, *21*(3), 1809–1825.
- Huete, A. R., Didan, K., Shimabukuro, Y. E., Ratanana, P., Saleska, S. R., Hutryra, L. R., et al. (2006). Amazon rainforests green-up with sunlight in dry season. *Geophysical Research Letters*, *33*, L06405. <https://doi.org/10.1029/2005GL025583>
- Hutryra, L. R., Munger, J. W., Saleska, S. R., Gottlieb, E., Daube, B. C., Dunn, A. L., et al. (2007). Seasonal controls on the exchange of carbon and water in an amazonian rain forest. *Journal of Geophysical Research*, *112*, G03008. <https://doi.org/10.1029/2006JG000365>
- Ivanov, V. Y., Hutryra, L. R., Wofsy, S. C., Munger, J. W., Saleska, S. R., Oliveira, R. C., & Camargo, P. B. (2012). Root niche separation can explain avoidance of seasonal drought stress and vulnerability of overstorey trees to extended drought in a mature amazonian forest. *Water Resources Research*, *48*, W12507. <https://doi.org/10.1029/2012WR011972>
- Joiner, J., Guanter, L., Lindstrot, R., Voigt, M., Vasilkov, A., Middleton, E., et al. (2013). Global monitoring of terrestrial chlorophyll fluorescence from moderate spectral resolution near-infrared satellite measurements: Methodology, simulations, and application to game-2. *Atmospheric Measurement Techniques*, *6*(2), 2803–2823.
- Kim, Y., Knox, R. G., Longo, M., Medvigy, D., Hutryra, L. R., Pyle, E. H., et al. (2012). Seasonal carbon dynamics and water fluxes in an Amazon rainforest. *Global Change Biology*, *18*(4), 1322–1334.
- Knox, R., Bisht, G., Wang, J., & Bras, R. (2011). Precipitation variability over the forest-to-nonforest transition in southwestern Amazonia. *Journal of Climate*, *24*(9), 2368–2377.
- Krinner, G., Viovy, N., de Noblet-Ducoudré, N., Ogée, J., Polcher, J., Friedlingstein, P., et al. (2005). A dynamic global vegetation model for studies of the coupled atmosphere-biosphere system. *Global Biogeochemical Cycles*, *19*, GB1015. <https://doi.org/10.1029/2003GB002199>
- Lee, J.-E., Berry, J. A., Tol, C., Yang, X., Guanter, L., Damm, A., et al. (2015). Simulations of chlorophyll fluorescence incorporated into the community land model version 4. *Global Change Biology*, *21*(9), 3469–3477.
- Lee, J.-E., Frankenberg, C., van der Tol, C., Berry, J. A., Guanter, L., Boyce, C. K., et al. (2013). Forest productivity and water stress in Amazonia: Observations from GOSAT chlorophyll fluorescence. *Proceedings of the Royal Society of London B: Biological Sciences*, *280*(1761), 20130171.
- Leuning, R. (1995). A critical appraisal of a combined stomatal-photosynthesis model for C3 plants. *Plant, Cell & Environment*, *18*(4), 339–355.
- Leuning, R., Van Gorsel, E., Massman, W. J., & Isaac, P. R. (2012). Reflections on the surface energy imbalance problem. *Agricultural and Forest Meteorology*, *156*, 65–74.
- Lewis, S. L., Brando, P. M., Phillips, O. L., van der Heijden, G. M., & Nepstad, D. (2011). The 2010 Amazon drought. *Science*, *331*(6017), 554–554.
- Lintner, B. R., Biasutti, M., Diffenbaugh, N. S., Lee, J.-E., Niznik, M. J., & Findell, K. L. (2012). Amplification of wet and dry month occurrence over tropical land regions in response to global warming. *Journal of Geophysical Research*, *117*, D11106. <https://doi.org/10.1029/2012JD017499>
- Liu, Y. Y., van Dijk, A. I., Miralles, D. G., McCabe, M. F., Evans, J. P., de Jeu, R. A., et al. (2018). Enhanced canopy growth precedes senescence in 2005 and 2010 amazonian droughts. *Remote Sensing of Environment*, *211*, 26–37.
- Machado, L., Laurent, H., Dessay, N., & Miranda, I. (2004). Seasonal and diurnal variability of convection over the Amazonia: A comparison of different vegetation types and large scale forcing. *Theoretical and Applied Climatology*, *78*(1-3), 61–77.
- Malhi, Y., Aragão, L. E., Galbraith, D., Huntingford, C., Fisher, R., Zelazowski, P., et al. (2009). Exploring the likelihood and mechanism of a climate-change-induced dieback of the amazon rainforest. *Proceedings of the National Academy of Sciences of the United States of America*, *106*(49), 20,610–20,615.
- Malhi, Y., Roberts, J. T., Betts, R. A., Killeen, T. J., Li, W., & Nobre, C. A. (2008). Climate change, deforestation, and the fate of the amazon. *Science*, *319*(5860), 169–172.
- Manoli, G., Meijide, A., Huth, N., Knohl, A., Kosugi, Y., Burlando, P., et al. (2018). Ecohydrological changes after tropical forest conversion to oil palm. *Environmental Research Letters*. <https://doi.org/10.1088/1748-9326/aac54e>
- Marengo, J. A., Tomasella, J., Alves, L. M., Soares, W. R., & Rodriguez, D. A. (2011). The drought of 2010 in the context of historical droughts in the amazon region. *Geophysical Research Letters*, *38*, L12703. <https://doi.org/10.1029/2011GL047436>
- Mastrotheodoros, T., Pappas, C., Molnar, P., Burlando, P., Keenan, T. F., Gentine, P., et al. (2017). Linking plant functional trait plasticity and the large increase in forest water use efficiency. *Journal of Geophysical Research: Biogeosciences*, *122*, 2393–2408. <https://doi.org/10.1002/2017JG003890>
- Meir, P., Brando, P. M., Nepstad, D., Vasconcelos, S., Costa, A., Davidson, E., et al. (2009). The effects of drought on amazonian rain forests. *Geophysical Monograph Series*, *186*, 429–449.
- Miguez-Macho, G., & Fan, Y. (2012). The role of groundwater in the amazon water cycle: 2. influence on seasonal soil moisture and evapotranspiration. *Journal of Geophysical Research*, *117*, D15113. <https://doi.org/10.1029/2012JD017540>
- Morton, D. C., Nagol, J., Carabajal, C. C., Rosette, J., Palace, M., Cook, B. D., et al. (2014). Amazon forests maintain consistent canopy structure and greenness during the dry season. *Nature*, *506*(7487), 221–224.
- Musavi, T., Migliavacca, M., Reichstein, M., Kattge, J., Wirth, C., Black, T. A., et al. (2017). Stand age and species richness dampen interannual variation of ecosystem-level photosynthetic capacity. *Nature Ecology & Evolution*, *1*, 0048.
- Myneni, R. B., Yang, W., Nemani, R. R., Huete, A. R., Dickinson, R. E., Knyazikhin, Y., et al. (2007). Large seasonal swings in leaf area of amazon rainforests. *Proceedings of the National Academy of Sciences of the United States of America*, *104*(12), 4820–4823.
- Nepstad, D. C., Tohver, I. M., Ray, D., Moutinho, P., & Cardinot, G. (2007). Mortality of large trees and lianas following experimental drought in an Amazon forest. *Ecology*, *88*(9), 2259–2269.
- Pappas, C., Fatichi, S., & Burlando, P. (2016). Modeling terrestrial carbon and water dynamics across climatic gradients: Does plant trait diversity matter? *New Phytologist*, *209*(1), 137–151.
- Paschalis, A., Fatichi, S., Katul, G. G., & Ivanov, V. Y. (2015). Cross-scale impact of climate temporal variability on ecosystem water and carbon fluxes. *Journal of Geophysical Research: Biogeosciences*, *120*(9), 1716–1740. <https://doi.org/10.1002/2015JG003002>
- Paschalis, A., Katul, G. G., Fatichi, S., Manoli, G., & Molnar, P. (2016). Matching ecohydrological processes and scales of banded vegetation patterns in semi-arid catchments. *Water Resources Research*, *52*, 2259–278. <https://doi.org/10.1002/2015WR017679>
- Phillips, O. L., Aragão, L. E., Lewis, S. L., Fisher, J. B., Lloyd, J., López-González, G., et al. (2009). Drought sensitivity of the Amazon rainforest. *Science*, *323*(5919), 1344–1347.
- Restrepo-Coupe, N., da Rocha, H. R., Hutryra, L. R., da Araujo, A. C., Borma, L. S., Christoffersen, B., et al. (2013). What drives the seasonality of photosynthesis across the Amazon basin? A cross-site analysis of eddy flux tower measurements from the Brasil flux network. *Agricultural and Forest Meteorology*, *182*, 128–144.
- Restrepo-Coupe, N., Levine, N. M., Christoffersen, B. O., Albert, L. P., Wu, J., Costa, M. H., et al. (2017). Do dynamic global vegetation models capture the seasonality of carbon fluxes in the Amazon basin? A data-model intercomparison. *Global Change Biology*, *23*(1), 191–208.

- Saleska, S. R., Didan, K., Huete, A. R., & Da Rocha, H. R. (2007). Amazon forests green-up during 2005 drought. *Science*, *318*(5850), 612–612.
- Saleska, S. R., Miller, S. D., Matross, D. M., Goulden, M. L., Wofsy, S. C., Da Rocha, H. R., et al. (2003). Carbon in Amazon forests: Unexpected seasonal fluxes and disturbance-induced losses. *Science*, *302*(5650), 1554–1557.
- Saleska, S. R., Wu, J., Guan, K., Araujo, A. C., Huete, A., Nobre, A. D., & Restrepo-Coupe, N. (2016). Dry-season greening of Amazon forests. *Nature*, *531*(7594), E4–E5.
- Samanta, A., Knyazikhin, Y., Xu, L., Dickinson, R. E., Fu, R., Costa, M. H., et al. (2012). Seasonal changes in leaf area of Amazon forests from leaf flushing and abscission. *Journal of Geophysical Research*, *117*, G01015. <https://doi.org/10.1029/2011JG001818>
- Saxton, K. E., & Rawls, W. J. (2006). Soil water characteristic estimates by texture and organic matter for hydrologic solutions. *Soil Science Society of America Journal*, *70*(5), 1569–1578.
- Schneider, U., Becker, A., Finger, P., Meyer-Christoffer, A., Rudolf, B., & Ziese, M. (2015). GPCC full data reanalysis version 7.0 at 0.5: Monthly land-surface precipitation from rain-gauges built on GTS-based and historic data. [https://doi.org/10.5676/DWD\\_GPCC/FD\\_M\\_V7\\_050](https://doi.org/10.5676/DWD_GPCC/FD_M_V7_050)
- Stark, S. C., Breshears, D. D., Garcia, E. S., Law, D. J., Minor, D. M., Saleska, S. R., et al. (2016). Toward accounting for ecoclimate teleconnections: Intra- and inter-continental consequences of altered energy balance after vegetation change. *Landscape Ecology*, *31*(1), 181–194.
- Verbeeck, H., Peylin, P., Bacour, C., Bonal, D., Steppe, K., & Ciais, P. (2011). Seasonal patterns of CO<sub>2</sub> fluxes in Amazon forests: Fusion of eddy covariance data and the orchidee model. *Journal of Geophysical Research*, *116*, G02018. <https://doi.org/10.1029/2010JG001544>
- Von Randow, C., Zeri, M., Restrepo-Coupe, N., Muza, M. N., de Gonçalves, L. G. G., Costa, M. H., et al. (2013). Inter-annual variability of carbon and water fluxes in Amazonian forest, Cerrado and pasture sites, as simulated by terrestrial biosphere models. *Agricultural and Forest Meteorology*, *182*, 145–155.
- Wright, J. S., Fu, R., Worden, J. R., Chakraborty, S., Clinton, N. E., Risi, C., et al. (2017). Rainforest-initiated wet season onset over the southern Amazon. *Proceedings of the National Academy of Sciences of the United States of America*, *114*(32), 8481–8486.
- Wright, S. J., & Van Schaik, C. P. (1994). Light and the phenology of tropical trees. *The American Naturalist*, *143*(1), 192–199.
- Wu, J., Albert, L. P., Lopes, A. P., Restrepo-Coupe, N., Hayek, M., Wiedemann, K. T., et al. (2016). Leaf development and demography explain photosynthetic seasonality in Amazon evergreen forests. *Science*, *351*(6276), 972–976.
- Wu, J., Guan, K., Hayek, M., Restrepo-Coupe, N., Wiedemann, K. T., Xu, X., et al. (2017). Partitioning controls on Amazon forest photosynthesis between environmental and biotic factors at hourly to interannual timescales. *Global Change Biology*, *23*(3), 1240–1257.
- Wu, J., Serbin, S. P., Xu, X., Albert, L. P., Chen, M., Meng, R., et al. (2017). The phenology of leaf quality and its within-canopy variation are essential for accurate modeling of photosynthesis in tropical evergreen forests. *Global Change Biology*, *23*, 4814–4827.
- Xu, X., Medvigy, D., Joseph Wright, S., Kitajima, K., Wu, J., Albert, L. P., et al. (2017). Variations of leaf longevity in tropical moist forests predicted by a trait-driven carbon optimality model. *Ecology Letters*, *20*(9), 1097–1106.
- Yang, X., Tang, J., Mustard, J. F., Lee, J.-E., Rossini, M., Joiner, J., et al. (2015). Solar-induced chlorophyll fluorescence that correlates with canopy photosynthesis on diurnal and seasonal scales in a temperate deciduous forest. *Geophysical Research Letters*, *42*, 2977–2987. <https://doi.org/10.1002/2015GL063201>
- Zhang, Y., Guanter, L., Berry, J. A., van der Tol, C., Yang, X., Tang, J., & Zhang, F. (2016). Model-based analysis of the relationship between sun-induced chlorophyll fluorescence and gross primary production for remote sensing applications. *Remote Sensing of Environment*, *187*, 145–155.
- Zhang, Y., Xiao, X., Jin, C., Dong, J., Zhou, S., Wagle, P., et al. (2016). Consistency between sun-induced chlorophyll fluorescence and gross primary production of vegetation in North America. *Remote Sensing of Environment*, *183*, 154–169.